APPENDIX A

NATURAL HAZARDS MONITORING: REMOTE SENSING OF VOLCANOS ACTIVITIES USING AN EXISTING FOREST FIRES MONITORING SYSTEM

INTRODUCTION

In the scientific landscape there are many existing Volcanoes monitoring systems which are working very accurately in order to detect, forecast and georeference the natural hazard [Kiyoshi Honda, Masahiko Nagai] due to the volcanoes activities.

In particular some of them are able to detect magma and lava movements(Sonia Calvari, Luigi Lodato and Letizia Spampinato), ash plumes and typology (Takahashi, Shoji), system able to distinguish lava flows and lava tubes, recognize storage of magma under the volcanoes, analyse active lava lakes (Flynn et al., 1993; Oppenheimer and Yirgu, 2002) and detect potential failure planes or fractures on recently formed cinder cones (Calvari and. Pinkerton, 2004) , etc.

These great amount of scientific results are done using several types of sensors from ground system or satellites system. The sensor mostly used are Thermal Camera, Visible Camera and NIR camera.

Regarding this project, it was decided to take advantage from existing remote sensing and monitoring systems in order to have a flexible, cheaper and very performance system.

It was tried to obtain the best trade-off between performance and cost, focusing on the suitability of the sensors and developing post-processing algorithms that could diminish any performance gap caused by the use of less sophisticated sensors. These sensors are less expensive and require low maintenance; factors that must be

taken strongly into account when talking about systems that work under the most adverse weather conditions.

The project is based on the infrastructure of SIRIO system, an existing early forest fires monitoring and detection system (Corgnati, Losso, Perona 2010). The performance and robustness of SIRIO have played an essential role for the choice, but also from the scientific point of view, it is necessary to say that the link between volcanoes and fires monitoring can be more closely than usually thought. For example heat sources of lava, hot-spot fires and ash smoke plume, smoke plume fires, etc, have an important relationship of the sensors utilized and post-processing algorithms developed in the natural hazard detection. Moreover, lava, magma and ash could be the possible outbreak of forest fires. All of these reasons, including simple architecture and robust to the hard environmental condition, led us to using that system for our purpose.

SIRIO is a ground-based image monitoring, is equipped by Thermocamera FLIR, handcamera, Reflex and a simple commercial camera. They can scan the frequency domain from visible to thermal. The system is also equipped by a motor which scan area of interest and it is able to make a wide shot every 4 to 10 minutes; the sampling time depends on the angle of scan and the motor speed settings.

The images are sent through internet connection to a remote server in which our algorithms work. The system could be able to arrange the type of connection, depending on the resources of the area where it works. For instance, it could be equipped by : Satellite, Cable or wireless ADSL, GPRS-EDGE-3G (using sim card), Wi-Fi, Wi-Max, etc.

The post-processing algorithms provide to identify the possible alarm due to hot-spot, smoke plume, lava etc. When an eruption is about to generate, the algorithms send an alarm to the operator safety which can manage the possible operations. Decision support algorithm, based on Digital Elevation Model (DEM), is able to link every single pixel of image with the geographical coordinates. In this way additional layers could be used for improve the operations as: helicopter

landing, water supply and squad location positions. These information, in case of needed, could be manage by operator through web interface.

Moreover, the system is equipped by a weather control unit which provides to obtain the data as: humidity, rainfall, direction and wind speed. These factors will be the key for the prediction, forecasting and detection of smoke plume and ash plume.

In order to adapt the system to volcanoes monitoring is necessary to locate a suitable place to avoid service interruptions caused by the effects of the volcano and fires.

Starting from the forest fires experience, volcanoes monitoring algorithms have been studied, adapted and developed. These algorithms could work together or distinctly if the operator decides by a faster or more sophisticated technique, obscuring and masking certain algorithms.

Basically, this shows us that the system is designed to have a lot of flexibility by using intelligence and human decision-making. Despite this, requiring only an initial calibration, the system can work and be strong even in a fully automatic way.

SENSORS

Volcanoes monitoring regard a number of activities involving heat detection as magma, lava flow, ash smoke, gas etc. A first stage of monitoring process could be performed by controlling one of these product as magma or lava hazard. For this reason, it was thought to use simple sensors such as cameras and video cameras, or more sophisticate monitoring sensors based on temperatures increased (thermocameras) or sensors which work on the infrared band.

The motivation for using these monitoring system is that the magma (and the heat source in general) has a unique emission spectrum due to the high temperature.

After briefly spectrum analysis and determining the wavelength which has the maximum emission of radiation, we could describe the thermocamera operation and finally we propose a monitoring model using this sensor.

It is necessary to know that none of these sensors (visible cameras, infrared cameras and thermocameras) are able to provide itself a complete and precise hazards monitoring. Could be necessary to combine the images, that these sensors provide and develop algorithms which can analyze and interpret the images in order to avoid false alarms and missed detections.

THERMAL MONITORING

In nature, all bodies whit a temperature greater the absolute zero, radiates according to the radiometry's law. In particular, if it is considered a black body, the irradiation is governed by the Plank's law. According to that it is possible to say that the magma is governed by this law as well.

A large part of energy transmitted by the magma is concentrated in a electromagnetic spectrum region between visible and thermal infrared. Using a Wien's law, it is able to estimate and calculate the value of wavelength at which the emission is maximum.

The electromagnetic spectrum is divided into several regions, ranked according to wavelength bands and named. In the electromagnetic spectrum, whole radiation are governed by the same laws and the only differences are those related to different wavelength (λ). The division of the EM (ElectroMagnetic) spectrum is shown in the table 8. The figure 17 shown us a graphical representation of the EM spectrum; enlargement is done in thermocamera sensitive region ($2 \div 13$ μm).

At this point, using the Wien's law (A.1) is possible to determine the wavelength corresponding to the magma maximum radiation.

$$T \cdot \lambda = b \qquad \text{(A.1)}$$

Where $b = 2{,}897 \cdot 10^{-3}\ [mK]$. To do that, it is necessary know the magma temperatures shown in the table 24.

Magma and heat source Typology	T max [°C]	Waveleght [μm]	Spectrum region
Magma Basaltic	1100	2	MIR
Magma Andestitic	1000	2.27	MIR
Rhyalitic Magma	800	2.7	MIR
Ash	390 ÷ 1000	2.27 ÷ 4.37	MIR

Table 24: Temperature of volcanoes hazard:

According to the values obtained, it is noted that all the highest emission generated by the magma and ash plume are concentrated in the MIR band.

Obviously it is not true to say that all the radiation produced by these heat source are concentrated in these areas of spectrum.

It is necessary to notice that the maximum is calculated in the ideal conditions, without take into account the air conditions which could prevent the propagation of radiation at certain wavelengths.

Since these, results show that the maximum radiation is located in the infrared domain, and for this reason could be used even sensors less expensive which operate (using particular filter lens) in the infrared band such as cameras and videocameras.

Monitoring lava and magma flow using an empiric model

Starting from forest fire models identification we developed an empiric lava flow monitoring and identification model. To do that it is necessary to determine minimum dimensions of lava flow and the instantaneous field of view of

thermocamera (IFOV), which represents a pixel displayed on the thermal map generated see chapter 2.

In the scientific landscape, the study of the dynamics of lava flows implies considering very complex aspects of multiphase materials such as physical and chemical heterogeneity and how they change over time and space (Griffiths, 2000). The models created are generally designed in order to take into account flow dynamics (Hulme, 1974; Ishihara et al., 1990; Baloga et al., 1995; Miyamoto e Sasaki, 1998; Tallarico e Dragoni, 2000), and cooling (Griffiths e Fink, 1993; Keszthelyi e Denlinger, 1996; Neri, 1998; Harris e Rowland, 2001; Patrick et al., 2004). These models are supported by numerous theoretical studies regarding morphology (Hulme, 1974; Dragoni et al., 1986; Baloga 1987; Crisp e Baloga 1990b; Wadge e Lopes, 1991). In addition to the viscosity, the final form of lava flow is controlled by the yield threshold (Hulme, 1974), volume erupted (Malin, 1980; Guest, et al., 1987), cooling (Crisp e Baloga 1990) and other parameters. The difficulties in lava flow modeling are also due to the considerable variability in the time of the parameters listed above; for instance, during cooling, there are considerable variations in temperature, the yield threshold and viscosity.

Therefore, it is not easy to study the effects that these parameters have on the lava flow morphology. An important goal for the volcanology landscape is to develop models to simulate the hazard.

Existing lava flows models can be divided into three main categories: deterministic, probabilistic and empirical. In our case we chose to use an empirical model. To model the lava flows we assumed to use the same methods and reasoning used for forest fire hot-spot detection adapted for our purpose and for our heat sources.

The point of that is to try to model lava, ash, smoke coming from the volcanoes according to a two dimensional geometry which models the size of the heat source in the early stage of the hazard. The value of dim_f is chosen in order to

obtain the best compromise between performance, false alarm rate and missed detection.

Regarding forest fire, the flame front model is described starting from the relationship between height and width flame under the classification of (Brown and Davis, 1973). According to this classification, the fire or generally the heat source, is classified according to various two dimensional geometry depending on the type of the observed object which we intend to identify. In order to model the lava flow it was thought to choose an appropriate geometry considering the external factor as gravity and slope of the volcano. The lava flow could be represent as rectangle due to these factors.

Since it is tried to identify and model the lava front at the early stage of its process, it is important to choose the best compromise between the size dim_f and the maximum distance at which the lava flows are able to be identified.

For that reason it is analyzed different size and dimensions; changing dim_f size, change the maximum distance at which the lava flows is identified as shown in the figure 62.

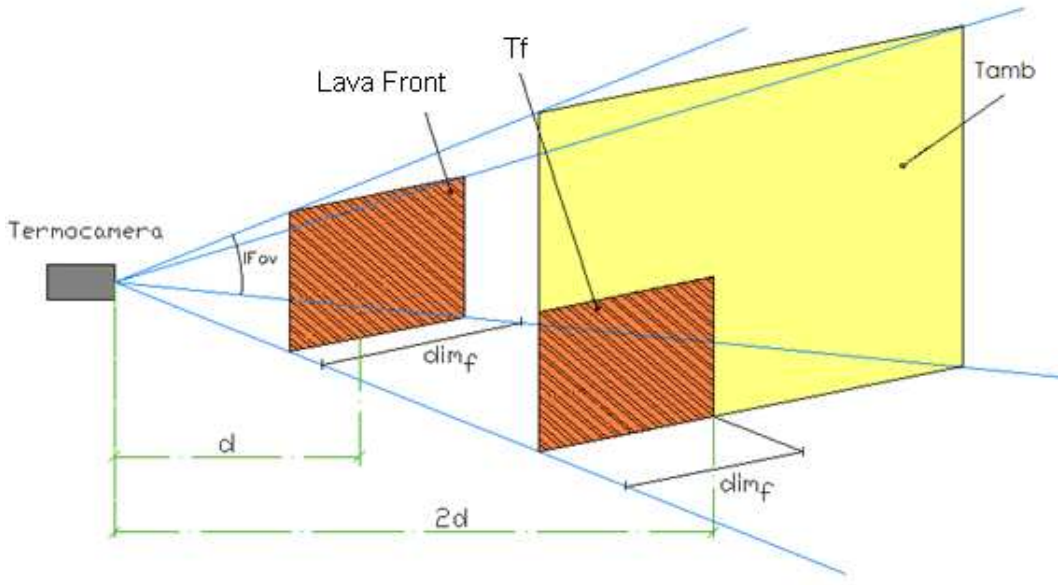

Figure 62 : model the lava front

Model results

The results are shown in the figures below. Considering several two dimensional geometry, environmental temperature equal to 20 °C, threshold temperature equal to 40°C, and the magma temperature shown in the table 24; it is possible to calculate the distance *d*, and the relative temperature, at which the size of heat source fall entirely within a thermal map pixel. After which it is calculated the maximum distance for the multiple of *d* (2*d, 3d*...) until the temperature is bigger than threshold temperature (40°C)

Basaltic Magma Tmax=1100 °C					
dim_f [mxm]	**Distance d [km]**	**Max distance [km]**	**Temperature[°C]**		
			d	***2d***	***3d***
1 x 0.5	0.769	3.8	560	155	80
2 x 1	1.54	7.7	560	155	80
3 x 2	2.31	13.8	740	200	100
4 x 3	3.01	18.5	830	222	110

Table 25: model results of Basaltic Magma

Andestitic Magma Tmax=1000 °C					
dim_f [mxm]	**Distance d [km]**	**Max distance [km]**	**Temperature[°C]**		
			d	***2d***	***3d***
1 x 0.5	0.769	3.7	510	142	74
2 x 1	1.54	7.5	510	142	74
3 x 2	2.31	13.5	673	183	92
4 x 3	3.01	18	755	203	101

Table 26: model results of Andestitic Magma

Rhyalitic Magma Tmax=800 °C					
dim_f [mxm]	**Distance d [km]**	**Max distance [km]**	**Temperature[°C]**		
			d	***2d***	***3d***
1 x 0.5	0.769	3.5	410	117	63
2 x 1	1.54	6.7	410	117	63
3 x 2	2.31	11.5	540	150	77
4 x 3	3.01	16.5	605	166	85

Table 27: model results of Rhyalitic Magma

Ash Tmin=390 °C					
dim_f [mxm]	**Distance d [km]**	**Max distance [km]**	**Temperature[°C]**		
			d	***2d***	***3d***
1 x 5	3.84	7	94	40	-
5 x 10	7.7	23	205	66	40
10 x 20	15	46	205	66	40
20 x 30	23	69	266	81	47

Table 28: model results of Ash

Considering the lava flow model, the dimension are smaller than the ash smoke. This is because the dynamic of the ash grow up faster than the lava flow due to the atmosphere and the environmental conditions.

It is necessary to consider that the results shown are take into account only the radiation due to the natural hazard. If it is considering the real radiation incident to the themocamera (atmosphere radiation), the maximum distance found will be slightly lower.

Thermal maps analysis for hot-spot and ash detection in the volcanic hazards

The goal is to develop an algorithm which is able to process and elaborate the temperature data and to obtain results as reliable and robust as possible. This algorithm could be divided in three main blocks as shown in the figure 63.

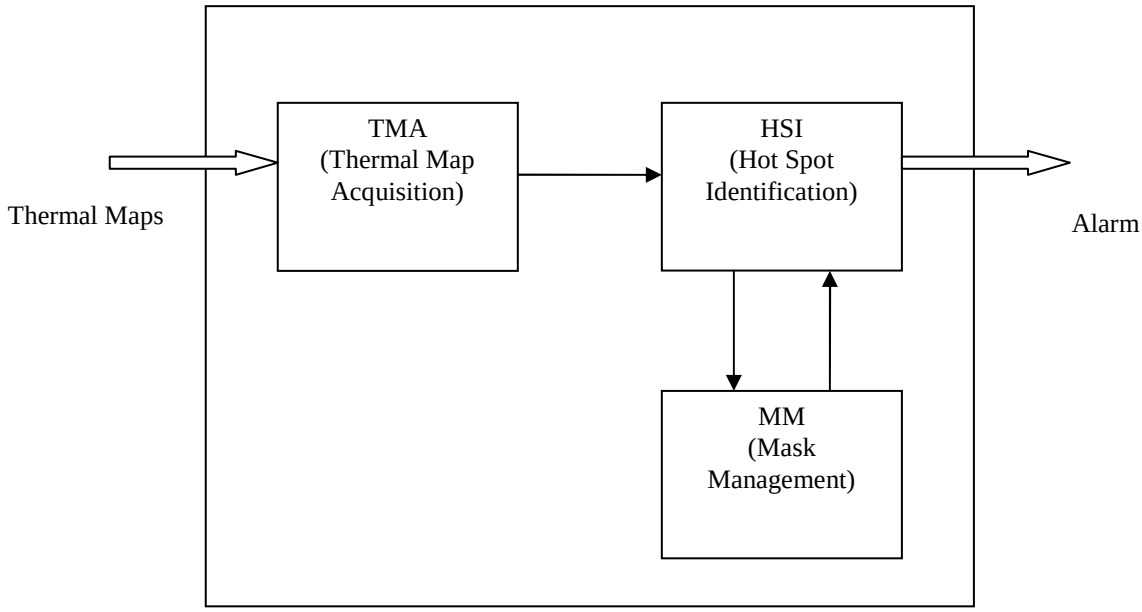

figure 63 : Hot-spot detection main blocks

TMA: Thermal Map Acquisition

The TMA block receives thermal maps from the thermal camera and turns into a format on which the following blocks can work without any problems. Thermal map is constituted as a matrix where every single cell (pixel) represents the average temperature detected by the sensor in the monitored area.

It is important to note that this average temperature depends on the distance from the sensor to the heat source as mentioned in the previous chapter.

For this reason it is not possible to monitor volcanoes slopes at a distance greater than the threshold value found in the thermal model tables (max distance).

This happened since the air layer between heat source and sensor does not allow to receive sufficient power to be detected by the sensor.

HSI: Hot-spot identification

The thermal maps acquired by TMA block are sent to the next block named HSI and are elaborated by the hot-spot algorithm.

Concerning hot-spot detection, it is considered an algorithm which detect sudden increases of temperature with respect to the threshold temperature set a priori.

Defining T_{MIN_FIRE} as the thermal threshold, T_{AMB} as the environmental temperature and DIM_{WIN} as the pixel's size processed: the lower boundary condition to consider the pixel as "event of fire" is represented by the following empiric relation:

$$T_{MEDIA} = \frac{8\left(T_{MIN\_FIRE} - 10\right) + \left(DIM^2_{WIN} - 8\right)T_{AMB} + T_{MIN\_FIRE}}{DIM^2_{WIN}} \qquad \text{(A.2)}$$

For each pixel, an arithmetic thermal average of DIM_{WIN} pixel has been considered around it. The thermal average must be bigger than (A.2) in order to recognize hot-spot pattern. When the block identified an hot-spot, HSI provides the alarm and the positions in which it was identifies.

MM: Mask Management

The monitored area could contain some features which reflect radiation and could produce false alarm during the hot-spot identification. These features as houses industrial buildings and so on, may be masked from processing because they are not relevant and significant to the identification.

MM block make possible the definition of areas in which the processing has to be masked. the function of the MM, however, is important because it allows to

reduce false alarm due to the environmental elements completely unrelated to a possible heat source.

VISIBLE MONITORING

The proposed system consists of additional sensors for environmental monitoring. In this case, the system used is also equipped with sensors able to scan the visible domain (and near-infrared using filters). These sensors are piloted by a motor which is able to scan the area of interest, making an overview, in the shortest time possible. The overview is composed in a RGB format (Red, Green, Blue).

Each pixel is the linear combination of RGB value, from this format it is possible to develop and adapt the post-processing algorithm to the images. In the scientific landscape, chromatic identification algorithms have been proposed for the identification of features such as : hot-spot, smoke, etc. The goal will be to make a feasibility study with existing algorithms and testing and developing new methods for volcanoes hazard identification.

Regarding hot-spot detection, exist some algorithms based on color features (Yunyang Yan; Zhibo Guo; Hongyan Wang 2009), fuzzy logic methods (SunJae Ham; ByoungChul Ko; JaeYeal Nam 2010) and statistical color methods (Celik, T.; Ozkaramanli, H.; Demirel, H. 2007). Other methods are based on decision function of fire-pixels is mainly deduced by the intensity and saturation.

Instead, concerning smoke detection algorithms used, they are mostly based on pattern recognition methods using : wavelet analysis (Yuan Wei , Yu Chunyu, Zhang Yongming 2009), color analysis between consecutive images (Losso, Corgnati, Perona 2011), statistical analysis of sample images (Turgay Çelik, Hüseyin Özkaramanlı, and Hasan Demirel 2007) and fuzzy logic methods (Wang, 2008).

Volcanoes ash identification is done using images sensed in the Lab format (particular format come from RGB). Regarding that, success algorithms and methods have already been proposed (Yuta Yamanoia, Shingo Takeuchib, 2007).

Lab image analysis for ash detection

A Lab color space is a color-component space with dimension L for lightness and a and b for the color-opponent dimensions, based on nonlinearly compressed CIE XYZ color space coordinates.

Unlike the RGB and CMYK color models, Lab color is designed to approximate human vision. It aspires to perceptual uniformity, and its L component closely matches human perception of lightness. It can thus be used to make accurate color balance corrections by modifying output curves in the a and b components, or to adjust the lightness contrast using the L component. In RGB or CMYK spaces, which model the output of physical devices rather than human visual perception, these transformations can only be done with the help of appropriate blend modes in the editing application.

It is possible to measure quantitatively colors of volcanic ash deposits erupted from three different styles of summit activity (Strombolian activity, Vulcanian explosions and continuous ash venting activity). Some studies have reported that they could be identify using the Lab domain. For instance, (Yamanoia ,Takeuchi 2008), Strombolian ash have larger yellow components of their visible spectra (b^* values) than those of explosion and continuous venting ash samples. Colors of explosion ash samples show larger variation in both red and yellow components of their visible spectra (a^* and b^* values, respectively), while colors of continuous venting ash samples are in the narrow ranges within colors of explosion ash samples.

the color variations of ash deposits are mainly originated from the particles composed of groundmass. The particles can be classified into three different types of particles with different viscosity and crystallinity (vesicular particle [VP], dense particle with vesicles [DPV] and dense particle without vesicles [DP]).

During the Strombolian activity, the VP is a main component in the ash. In the Vulcanian explosion and continuous ash venting activity, the proportions of DPV and DP in ash are larger than that in the Strombolian activity.

RGB analysis smoke detection in the volcanic hazards

As shown in the Figure 6, the algorithm for smoke detection is based on two principal blocks: the first calculating different chromatic changes (called static block) and the second calculating the correlation spatial and temporal patterns (called dynamic block).

Before carrying out the process it is necessary to “binarize” the images, by dividing into regions or bin the pixels of the images. Basically, the Bin is a large pixel composed by several pixel. The dimension of it is defined a priori by the operator. Each bin value is represented by mean value of its pixel. The dimension of the bin depends on the resolution of the images and it is chosen to tracks the dynamic of the smoke as well as possible.

Smoke detection Algorithm is discussed in the chapter 3, the results obtained are processed by other algorithm which are able to determine other feature (as Volume and speed). That will discuss in the next Chapter.

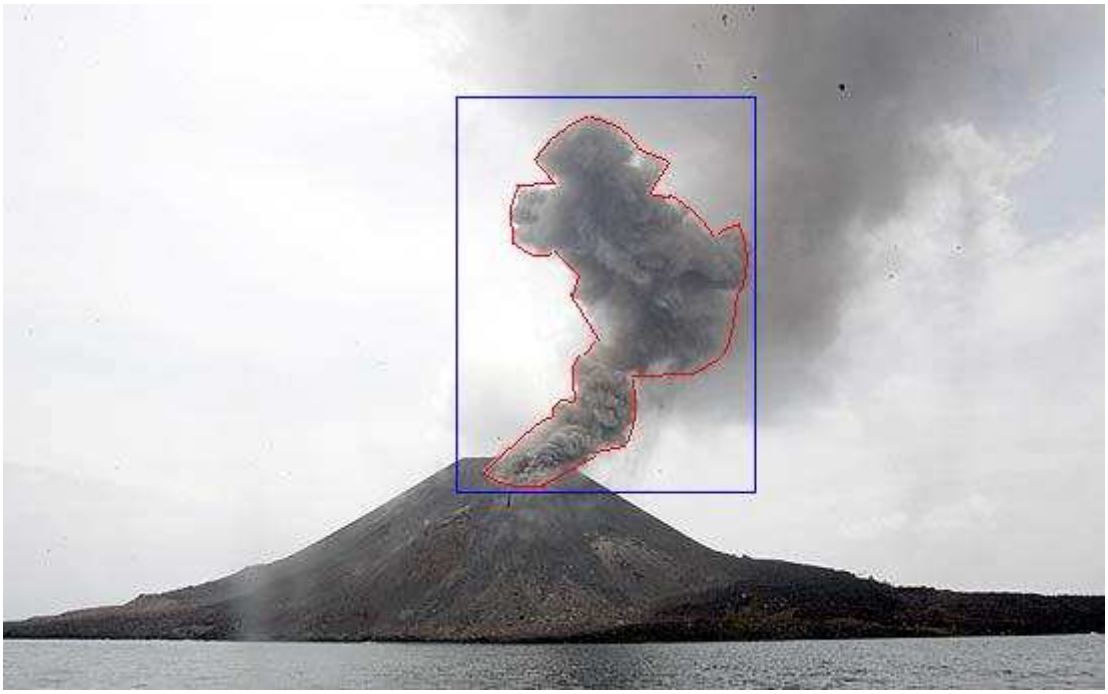

Figure 64 : smoke pattern found

Ash Speed and Volume Detection

Using the sensors and the algorithms discussed before; it is possible to develop a new algorithm which is able to calculate the ash speed and the Volume. This is done using the smoke detection algorithm which include the pattern recognition method. The pattern found is able to identify the surface of the smoke/ash in term of number of pixels. In order to determine the speed of the ash plume and to determine a possible forecasting of its dynamic it is needed to calculate the volume. The volume V is defined as:

$$V = \text{Height} \times \text{Width} \times \text{Length} \qquad \text{(A.3)}$$

Using only one sensor is possible to calculate only two dimension (Height and Width), in this case, knowing the number of pixels which belong to the pattern, just two-dimensional surface could be estimate. It is necessary to obtain the other feature and this could be guaranteed using a new system located where its sensor's field of view design a 90° angle respect to the other. This is shown in the figure 65.

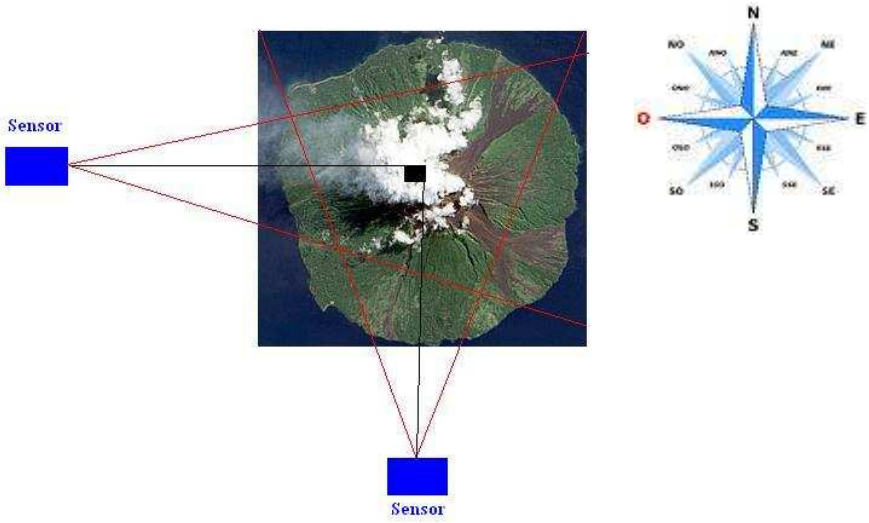

Figure 65: sensors position

In this case, the same smoke algorithm provides to calculate the ash plume pattern and to determine the Volume knowing the remaining feature. In the figure 66 is shown a possible example.

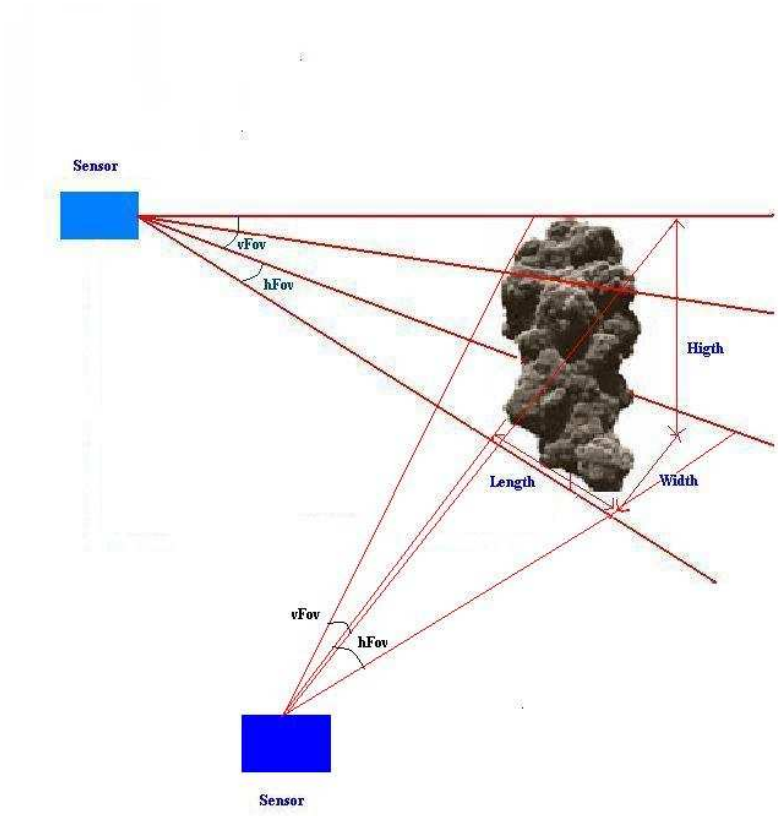

Figure 66 : 3d sensor position and features (width, high, length)

Since to the smoke detection pattern we are able to determine and estimate the speed of the ash and volume dynamic. As mentioned, smoke detection is done comparing a reference image with another image.

The results, as smoke patterns (or ash in this case), are able to compared between themselves in order to estimate the dynamic, the speed and the direction of ash plume as well.

First of all, according to the pattern recognition method, it was identified the ash plume as a geometric figure constituted by several pixels. As shown in figures 67-68, it is possible to calculate the surface area, calculating the number of pixel in the pattern shown below.

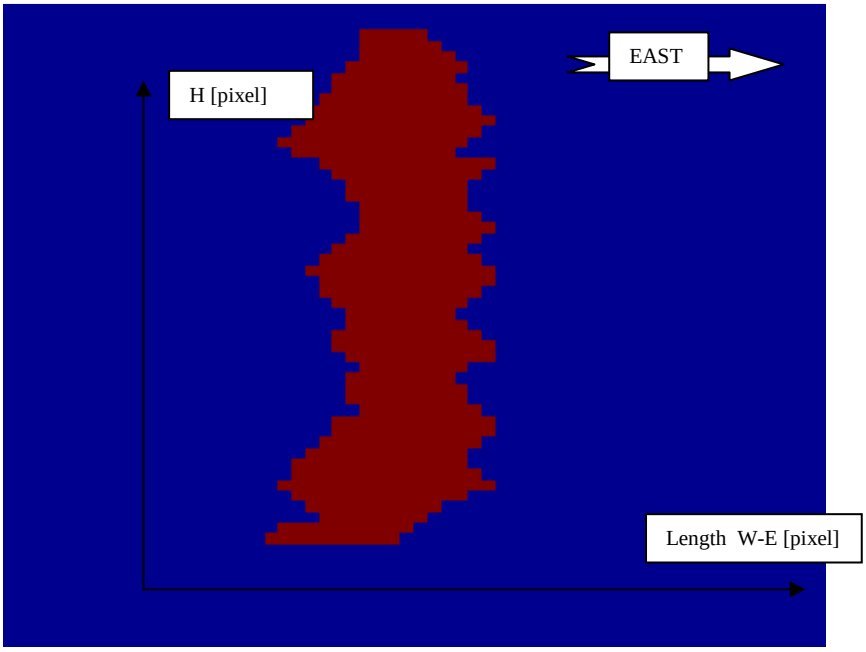

Figure 67: West – East pattern

The same proceeding is done using the other sensor and using the same algorithm in the mean time is possible to carried out the other pattern.

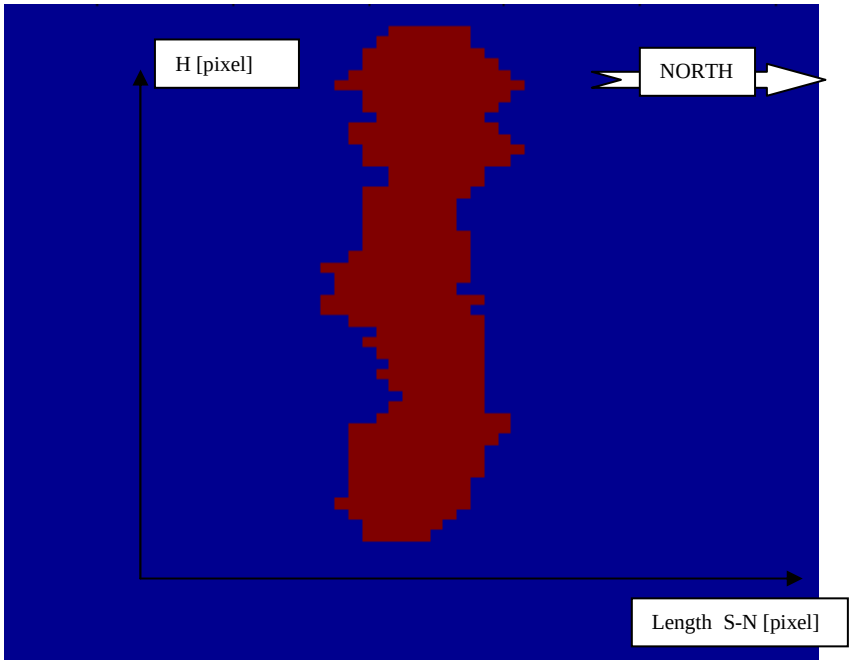

Figure 68: North – South pattern

As mentioned, knowing both of patterns, it is able to calculate the ash volume according to the relation:

$$V = \text{High} \times \text{Width} \times \text{Length [pixel]} \qquad \text{(A.4)}$$

The value found will be represented in pixel, in the next chapter will be described the method to calculate the volume in m^3.

After that, the smoke detection, it is able to identify the next pattern according to the next image acquisition. As mentioned the time schedule could be manage a priori in order to obtain the best compromise between early detection and processing time. In the figures 69 -70 is shown what happen if the smoke detection algorithm identify another pattern after the new acquisition from the sensor. The pattern colored as blue is the first pattern, while the red one is the second in term of time detection. It is possible to see the movement of the ash respect to the previous position. It this case it is easily to calculate the movement in term of pixels.

In order to calculate the ash Volume and other feature as: speed, direction, etc, it was utilized two sensor located 90 ° between themselves as mentioned before, one of this is placed in way to obtain a perpendicular angle with the North-South line and the other one placed to obtain a perpendicular angle with the East-West line. The main idea is shown in the figure 67, The figure 69 could be represent the pattern identified from the East-West sensor.

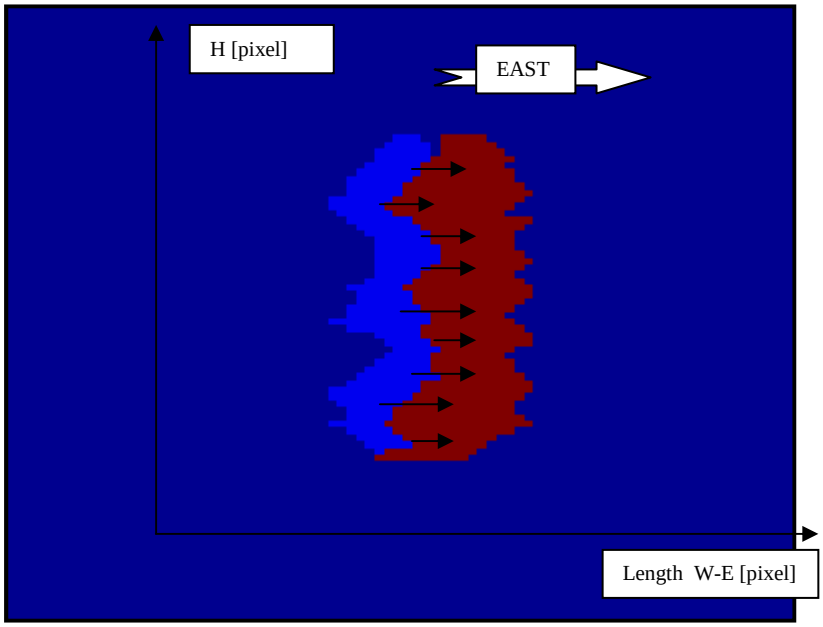

Figure 69: West-East pattern movement

In the mean time the other sensor is able to detect the North-South pattern in way to obtain the feature to calculate the Volume and the ash speed. This is an example of pattern identified in the North-South line.

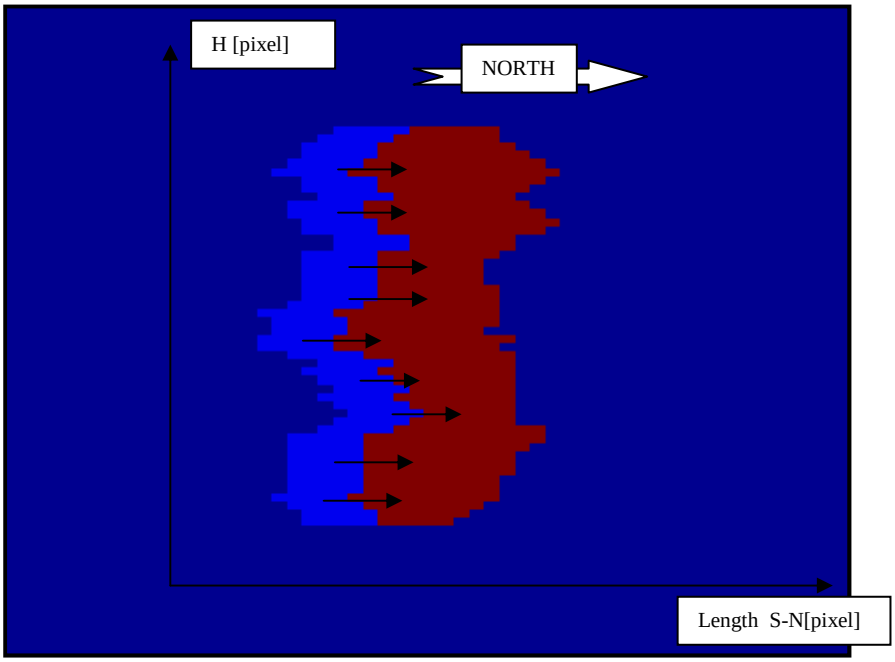

Figure 70: North-South pattern movement

The arrows shown in the figure 71 represent the displacement of the pixels between two consecutive images. Knowing the displacement in term of pixel, it possible to calculate the ash speed in term of pixel as well. The well-being will be to calculate for every pixel the displacement and the moving result is the average of this values, but it is possible to simplify the processing taking into account the arrow which has the maximum value.

Before to carried out the resultant of both of speed (North-South, East-West) is necessary to say that it was taken into account the vector (arrow) which are parallel with the x-axis and parallel with the surface. This represent another simplification from the real world because the pixel movement could be yield due to the wind, which is not necessary parallel to the surface. This assumption could be taking into account especially if the timing between two images is short as possible. At this point it is possible to calculate the movement in term of pixel from both sensors.

It is displayed the speed vectors (Vn and Ve, respectively North speed and East speed) in a graphic in order to obtain the resultant speed vector Vr. The example is shown in the figure 71.

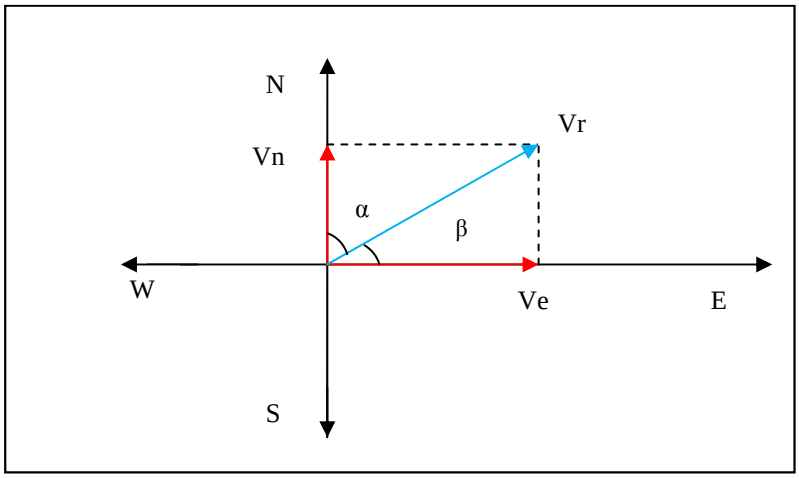

Figure 71 : displacement of the pixels (North-South, East-West)

The speed value corresponds to the vector Vr, which is calculated according trigonometric law (Pitagora's Law) in term of pixel. The formula will be

$$Ve^2 + Vn^2 = Vr^2$$

At this point it could know the ash Volume and the ash movement, it remains to calculate the direction of the ash the speed.

For the first issue, it necessary to know in which direction the patterns, from both sensors, are moved. In the example shown in the figure 71, if it is recognized the movement to East from the first sensor and to North from the other sensor, it is necessary to say that the total ash direction is North-East. If it is calculated the angle movement respect to the North is necessary to know the angle α.

$$\beta = arcsen\ \frac{Vn}{Vr}$$

$$\alpha = 90° - \beta$$

Before carried out the meter value of the movement between two consecutives images, it was introduced an additional tool in order to link the pixel value of the vector Vr to the meter value.

This additional tool is named DEM (Digital Elavation Model) and represent the digital surface of the areas which it is intended to monitor. Every single pixel of the DEM is linked with a geographical coordinates and because of that, we are able to calculate the distance (in meter or in degree) between two pixel. It is easy and cheaper to obtain a DEM as reliable as possible, in the scientific landscape exist some of them with resolution about 15 meters or even less. The main idea of proceeding is represented in the next chapter.

Geo-referencing tool and ash speed measurement

Geo-referencing method

Geo-referencing tool is based on projective and geometric methods in order to achieve the best geographical linking trade-off (Losso, Corgnati, Perona 2010). Elevation profile and geographical information are extracted from the cone of view on DEM; see chapter 3 for geo-referencing methods.

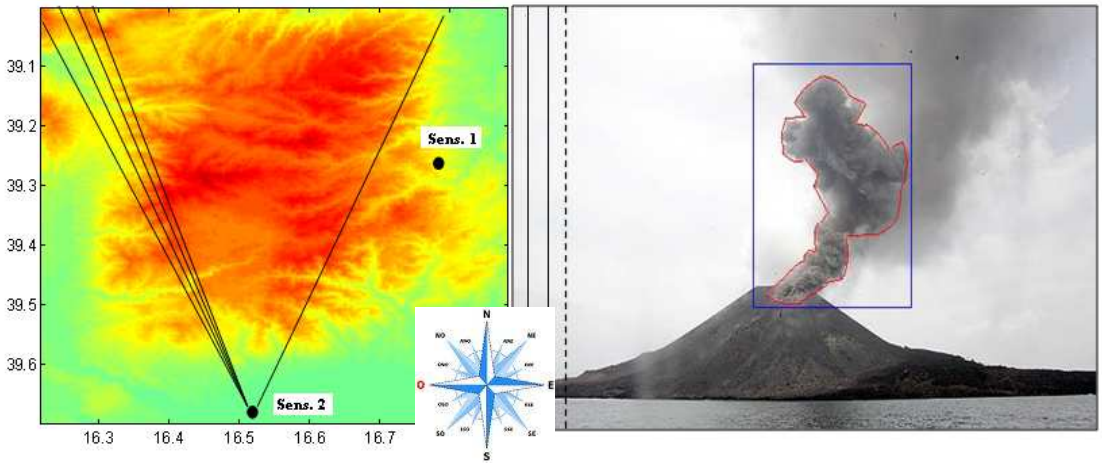

Figure 72: (a) Example of field of view portion considered on image (b) Example of horizon field of view portion considered

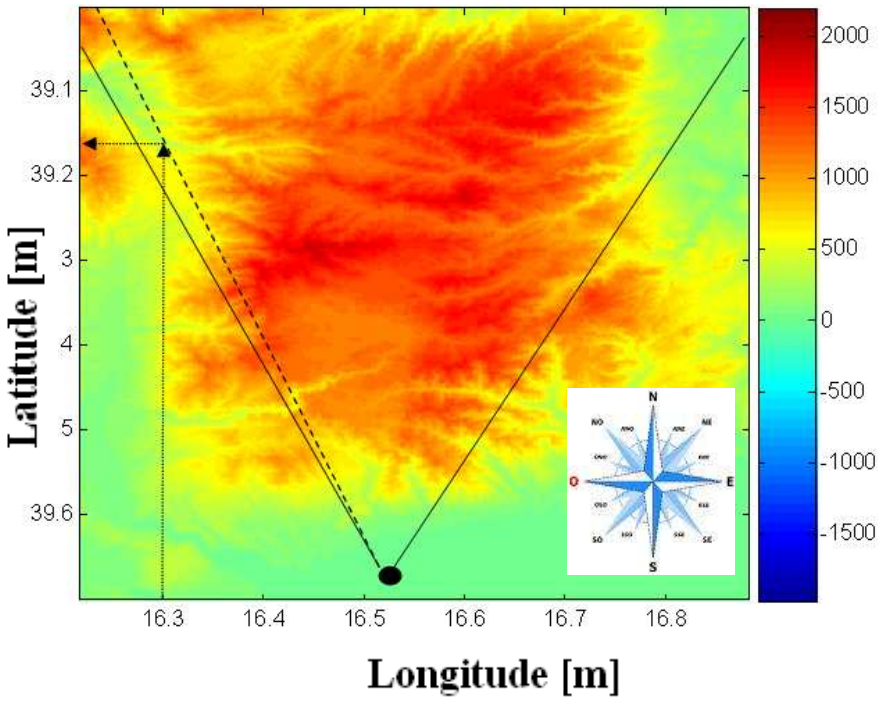

Figure 73: Determining the latitude component

In this way we can obtain a matrix which has the same pixel number of the original image. Every pixel has linked with a geographical coordinate in term of

meters (UTM coordinates). At this point, it is possible to link every single pixel movement found out of the ash to the relative geographical position, then it is able to find out the meters movement of the ash. The same procedure is done for the other sensor.

ASH VOLUME

In order to measure the ash Volume in term of m^3, georeferencing is needed to the image, as mentioned in the previous chapter. Just for example, we could fix the features found using the pattern as:

Width [pixel]	High [pixel]	Length [pixel]
20	40	30

Table 29: pixel value of the pattern found

The image NxM geo-referenced is a matrix NxM where each pixel is linked with a geographical coordinate in term of meter (UTM). The volcano vent position is know on the image, so it is possible to fix the exactly geographical position. From this value the pixel distance of the features (Width, High, Length) is known, using the geo-referenced matrix, the difference (in term of meters) between the origin (volcano vent) and every single ash feature is calculated. According to the Hight it is needed to know the vent and the ash altitude, but using the DEM these information are obtained as well as the width and length.

After that, it is possible to convert the pixel values, of the features, in meters, as mentioned before. For example :

Width [meters]	High [meters]	Length [meters]
30	50	25

Table 30: pixel values convert in meters

The volume in m^3 is calculated according to the approximate formula shown below:

$$V = \text{High x Width x Length } [m^3] \quad \text{(A.5)}$$

Where V = 50 x 30 x 25 = 37500 $[m^3]$

ASH SPEED MEASUREMENT

As mentioned, knowing for each image pixel the geographical value is possible to know the ash movement in term of meters, the pixel movement is represented in the figure 74.

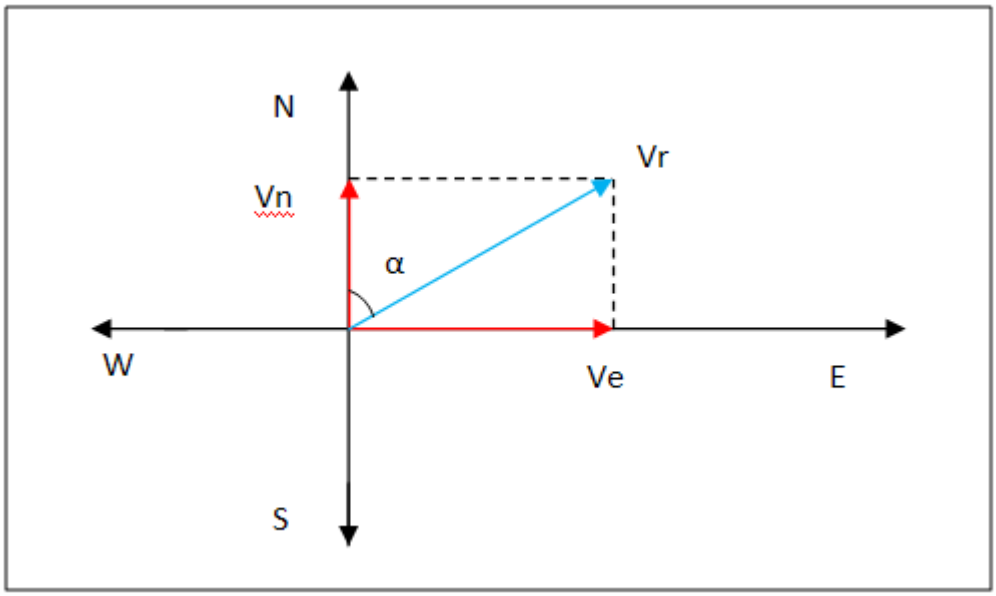

Figure 74 : displacement of the pixels (North-South, East-West)

The arrows Vn and Ve will be placed at the origin of the volcano vent and Vr (in meter) will be obtained using :

$$Ve^2 + Vn^2 = Vr^2 \quad \text{(A.6)}$$

For example, if the value of Ve is equal to 3 pixel and the value of Vn is 2 pixel, it necessary to convert this values as meters according to the previous image geo-referencing method. The values of this pixel is linked to the values found in the matrix obtained considering as origin the volcano vent. The distance is calculated as the difference between two geographical coordinates (first pixel – last pixel). The first pixel will be the volcano vent (the origin); from this pixel it is taken into account 3 pixel (Ve) and 2 pixel (Vn). Just for example, in term of meters, it was found out 45m of East movement and 30m of North movement. The direction of the ash speed will be North-East, and the Vr value, according with the relation, will be :

$$45^2 + 30^2 = Vr^2$$

The value of Vr in this example will be equal to 45,1 meters. This means that between two consecutives images the ash movement has traveled about 45,1 meters in the N-E direction with an angle equal to α.

This angle as mentioned before, is calculated according with this relation:

$$\beta = arcsen\ \frac{Vn}{Vr} \tag{A.7}$$

$$\alpha = 90° - \beta$$

Therefore the angle α respect to the North will be :

$$\beta = arcsen\ \frac{30}{45.1} = 0.73\ [rad]$$

Before carried out the value of α is necessary to convert the $[rad]$ value into $[deg]$ value. This is done according the simply expression :

(A.8)

Therefore, in term of degree will be :

Where is the new value of in degree. At this point is simple to calculate the angle respect to the North, which will be:

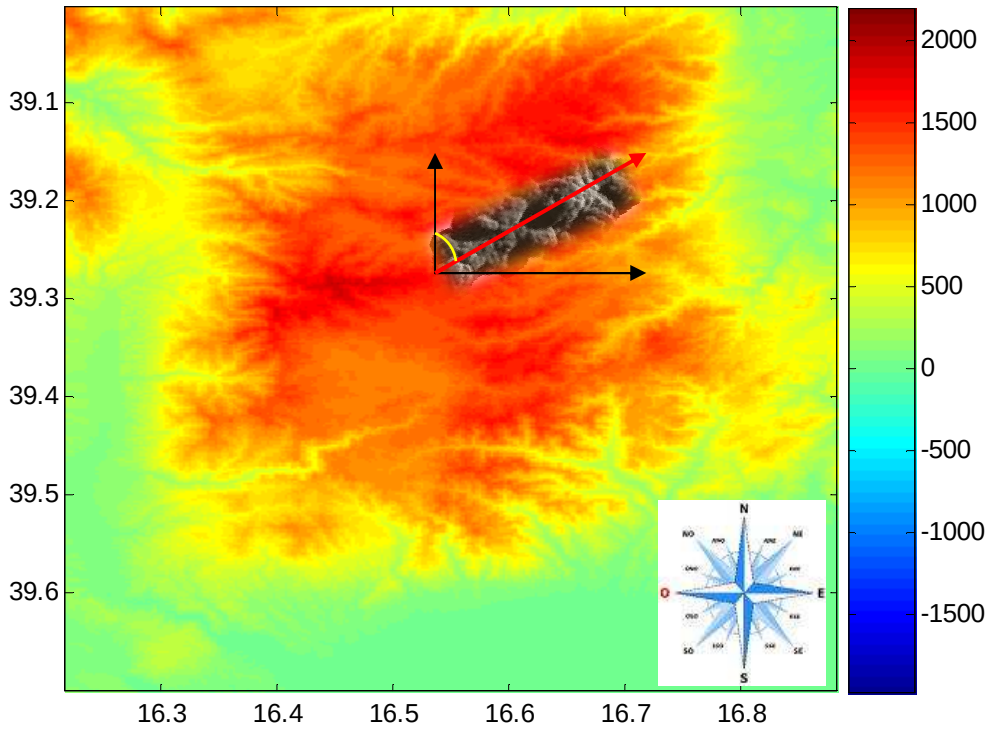

Figure 75 : horizontal ash speed on DEM

Regarding the measurement of ash speed v, it is calculated according to the simply relation :

$$v = \frac{s}{t} \quad [\frac{m}{s}]$$

where *s* is the distance express in meter and *t* represent the time. The distance *s*, according to the previous example is 45,1 [m] and the time *t* is the timing between two consecutive images, it is set by operator and is possible to know it a priori. For example if it is set it as 1 minute (60 seconds), the ash speed will be :

$$v = \frac{45{,}1}{60} = 0.751 \ [\frac{m}{s}]$$

In term of *Km/h* that value will be $0.751 \ \left[\frac{m}{s}\right] * \ 3.6 = 2.7 \ \left[\frac{km}{h}\right]$.

The results depend on the DEM resolution; in this case it could be obtained a maximum error equal to the pixel resolution. The origin, for each pixel, is considered as the centre of pixel, that means that the error which could be commit is half pixel for the first one and half pixel for the last. This could be represented in the figure below:

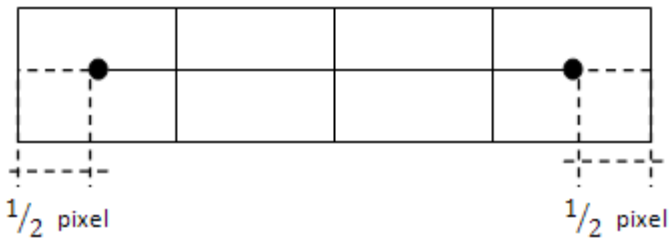

Figure 76 : maximum error

Just to simplify, the results are carried out taking into account only the horizontal movement of the wind. A real situation could be composed as : horizontal

or vertical or both of them. Therefore , it is also necessary to analyze the other type of movement.

Vertical ash

In case of vertical ash the previous proceeding could be take into account with just few adjustment. When there is absence of wind (<1 —) , the ash goes only through the sky in vertical way. This means that during the smoke detection processing, the pixel pattern between two consecutive image goes through the top of the image. The way to proceed is quite the same to the previous. As mentioned, the pattern is detected as well as the difference between the images (if there are). This is shown the figure 77:

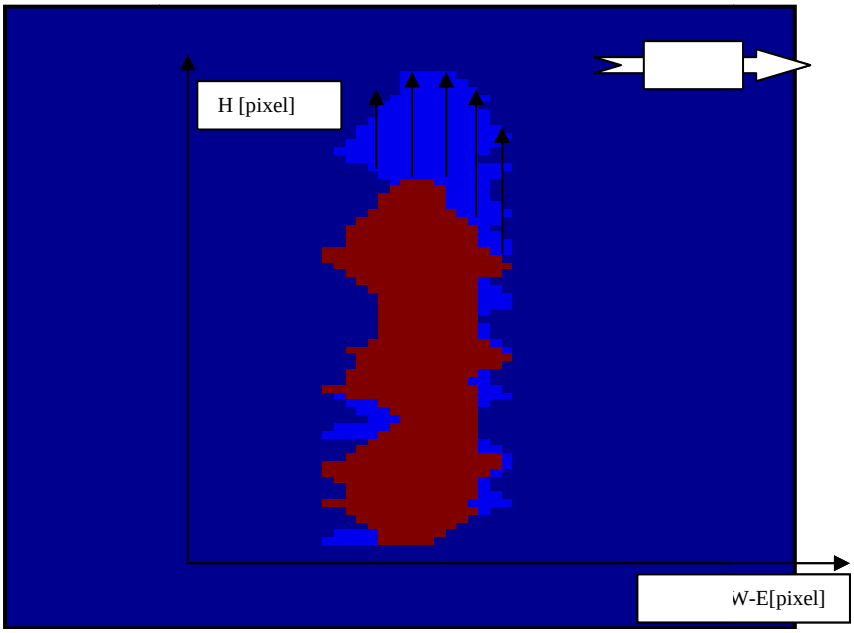

Figure 77 : Vertical ash movement

In the mean time the other sensor is able to detect the North-South pattern in way to obtain the feature to calculate the Volume and the ash speed.

Knowing the movement, in term of pixel, it is possible to calculate the movement in term of meters as mentioned before. It is necessary to know the altitude

from the vent (origin) and the top of the ash using the geo-referencing tool. As for example, 4 pixel of movement represent, according to the altitude difference, 20 meters. The speed is calculated knowing the timing between two consecutive images, for example if we set it as 1 minute (60 seconds), the ash speed will be :

$$v = \frac{20}{60} = 0.33 \ [\frac{m}{s}]$$

Vertical and horizontal Ash (real case)

At this point it is able to measure and calculate the full contribute, in term of vertical and horizontal ash. Considering the full contribute, the ash movement is calculated knowing the movement (in pixel or in meters) calculated separately as in the previous examples. As shown in the figure 78, the arrow V_1 represents the vertical ash movement and the arrow V_2 represent the horizontal ash movement according to the relative direction (N-E); the result is shown as arrow V_3 and its value is calculated using Pitagora's Law :

$$V_1{}^2 + V_2{}^2 = V_3{}^2$$

Where V_1 is equal to 20 meters and V_2 is equal to 45,1 meters. According to these values V_3 is:

$$V_3{}^2 = 20^2 + 45{,}1^2 = 49.33 \text{ m}$$

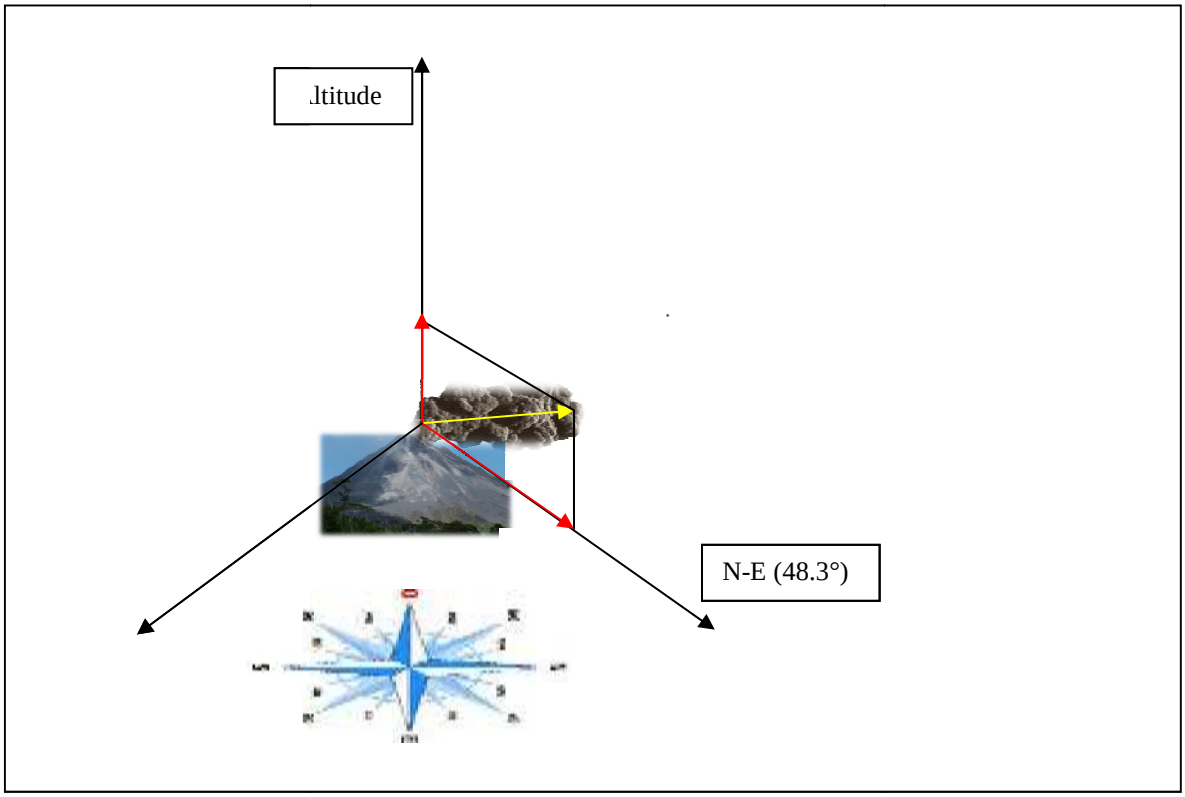

Figure 78 : vertical and horizontal Ash (real case), total contribution and result

The direction is the same, 48.3° from the North (North – East). Considering the timing equal to 60 seconds between two consecutive images, the full component speed is :

— —

In term of *Km/h* that value will be — — .

MAGMA SPEED MEASUREMENT

Concerning the Magma detection, as mentioned, it is possible to detect it using the hot-spot algorithm. Since the algorithm provide to show the result as pattern (in this case magma pattern); it was used the same proceeding, described previously, in order to evaluate the magma speed, and if it is possible to forecast the possible magma path along the volcano surface. It is necessary to use a DEM with resolution as high as possible to evaluate with precision the speed and the forecasting.

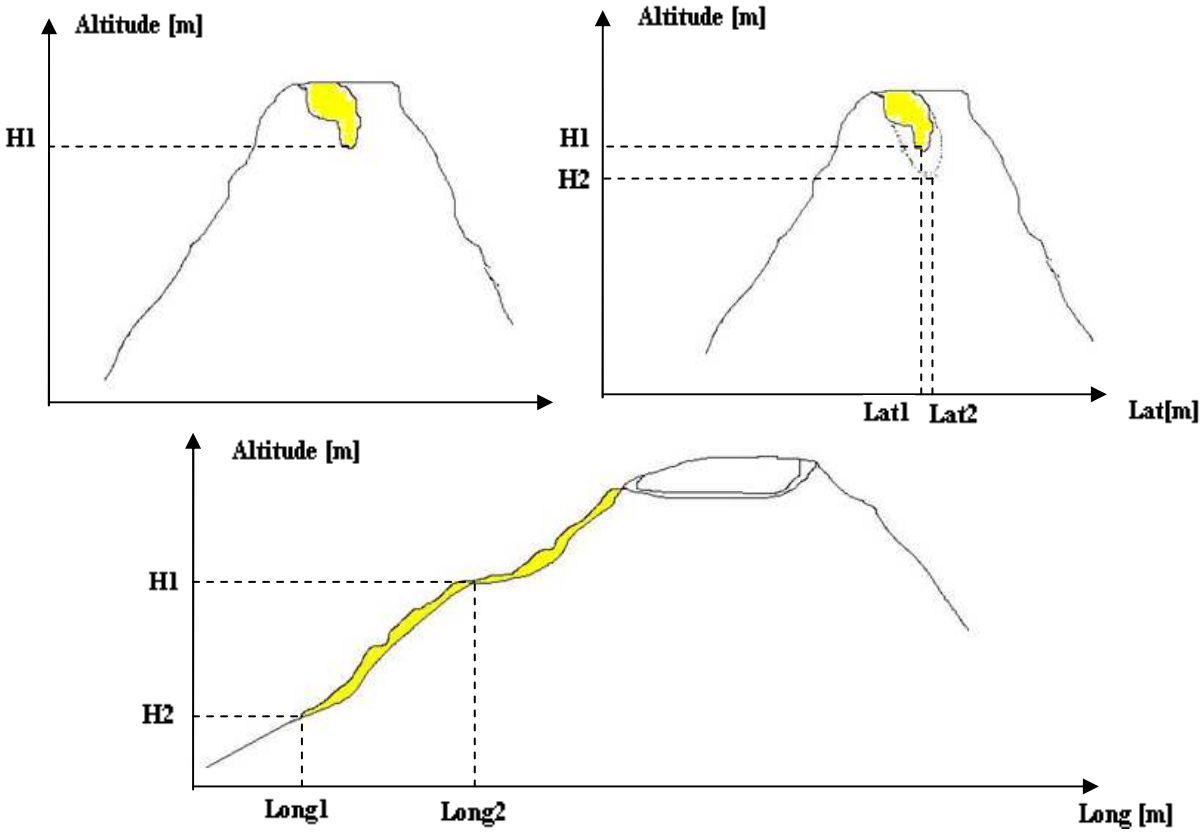

Figure 79: example of lava speed measurement

In the figure 79, is shown an example of lava speed measurement. At the first time, a thermal map is taken from the sensor and the hot-spot algorithm detects the pattern. Since from that, it is able to localize, in term of pixel, the position of the lower pixel and according to the DEM, the altitude H1 and the latitude could be obtained as well. Remember that the thermal map could be geo-referenced as well as the RGB images.

The other sensor placed at 90 ° from the first one, is able to detect, in the same way to the previous, the Longitude position of H1. After a certain time set by the operator, the second thermal map is taken making possible the detection from both sensors. If the position of the lower point of the lava flow is different respect the previous one, it is possible to calculate the new altitude, H2, and the geographical coordinates (latitude and longitude) of this point. The speed is calculated as:

$$v = \frac{s}{t} \quad [\frac{m}{s}]$$

The time *t* is the timing between two consecutives images, while the distance *s* is calculated using the geographical position in meters (latitude and longitude) and a simple Pitagora's Law. Furthermore it was obtained the rise in percentage as:

$$rise = \frac{|H1 - H2|}{H1} * 100\ [\%] \qquad (A.9)$$

After 2 images is possible to determine the average of acceleration, the formula will be:

$$a = \frac{v2 - v1}{t2 - t1} \qquad (A.10)$$

Where *v2* is the speed at the time instant *t2*, while *v1* is the speed at the time instant *t1*. For instance, after the DEM measurement is possible to find H1 = 2000m and H2 = 1900m and the timing is 60 seconds. The speed will be:

$$v = \frac{100}{60} \quad = 1.66\ [\frac{m}{s}]$$

The rise will be:

$$rise = \frac{|2000 - 1900|}{2000} * \ 100 = \ 5\%$$

After another acquisition, if the speed v2 is equal to the previous speed v1, the acceleration will be equal to 0.

CONCLUSION & FUTURE WORK

A system for volcanoes monitoring , based on thermo cameras and commercial sensor has been proposed. A model of lava flow is developed in order to knowing a priori the distance at which the thermocamera could detect the lava pattern on the volcanoes surface. This is an important fact because allow to place the sensors at certain distance from the volcanoes vent, in order to preserve the sensors to the environmental condition and to the volcanoes hazards; furthermore, in the mean time, it is possible to obtain result as reliable as possible. Combining radiometric analyses, image graphical and motion processing the system can detect lava flow and ash plumes patterns due to volcanoes hazards within time intervals of few minutes with a precise spatial location. Using systems placed at 90° from

themselves, ash features as: volume, speed and direction can be measured as well as the lava features as: speed and acceleration. A Digital Elevation Model (DEM) with high resolution is able to link every single image and thermal map pixel with a geographical position (latitude and longitude) in term of meters. In this case, volume, speed and direction could be obtain using consecutive images. At the moment, our primary target is the successfully implementation of the algorithms using thermal maps and visible images.

Future target will be the systems installation in a test area, we could suggest the Etna Volcanoes because is always active but it is not too much dangerous. Even the Etna orography could allow us to obtain good results. Afterwards we could develop forecasting algorithm for ash and lava flow using consecutive images and a forecast control unit. The algorithms are operating for test activities onboard the integrated monitoring system for high performance decision support SIRIO (Sistema Integrato per il Rilevamento di Incendi bOschivi) developed by EST S.r.l. and SVM S.r.l.

References for Volcanoes Hazard monitoring

Baloga, S., (1987), Lava flows as kinematic waves, J. Geophys. Res., 92, 9271-9279.

Berni J., Galán R, González L. 2008. A vision-based monitoring system for very early automatic detection of forest fires. Modeling, Monitoring and Management of Forest Fires I.

Brown, Arthur A; David, Kenneth P. 1973. Forest fire control and use, 2nd edition. New York,NY: McGraw-Hill. 686 p.

Calvari, S., and H. Pinkerton (2004), Birth, growth and morphologic evolution of the ‘‘Laghetto’’ cinder cone during the 2001 Etna eruption, J. Volcanol. Geotherm. Res., 132, 225 – 239, doi :10.1016/S0377-0273(03)00347-0.

Calvari S, Lodato L, and Spampinato L., 2004. Monitoring active volcanoes using a handheld thermal camera.

Celik, T.; Ozkaramanli, H.; Demirel, H. 2007. Fire detection using statistical color model in video sequences
Journal of Visual Communication and Image Representation Volume 18 Issue 2, April, 2007

Corgnati L., Losso A., Perona G. 2010. SIRIO high performance decision support system for wildfire fighting in alpine regions: an integrated system for risk forecasting and monitoring. Forest fires II, Kos Greece.

Crisp, J. e S. Baloga, (1990a). A method for estimating eruption rates of planetary lava flows, Icarus, 85:512-515

Flynn, L. P., P. J. Mouginis-Mark, J. C. Gradie, and P. G. Lucey (1993), Radiative temperature measurements at Kupaianaha Lava Lake, Kilauea Volcano, Hawaii, J. Geophys. Res., 98, 6461 – 6476.

Griffiths, R.W., (2000). The dynamics of lava flows, Annual Review of Fluid Mechanics 32, 477–518.

Griffiths, R.W., e J.H. Fink (1993), Effects of surface cooling on the spreading of lava flows and domes, J. Fluid Mech., 252, 667– 702.

Guest, J.E., C.R.J. Kilburn, H. Pinkerton, e A.M. Duncan, (1987), The evolution of lava flow-fields: observations of the 1981 and 1983 eruptions of Mount Etna, Sicily, Bull. Volcanol. 49, 527– 540

Harris, A.J.L., e S.K. Rowland (2001), FLOWGO: A kinematic thermheological model for lava flowing in a channel, Bull. Volcanol., 63, 20–44.

Hulme G., (1974). The interpretation of lava flow morphology, Geophys. J. Roy. Astro. Soc. 39: pp. 361.

Ishihara, K., M. Iguchi, e K. Kamo (1990), Numerical simulation of lava flows on some volcanoes in Japan, in: Lava Flows and Domes: Emplacement Mechanisms and Hazard Implications, edited by: Fink, J. K (Springer, Berlin), 174–207, 1990.

Keszthelyi, L., e R. Denlinger (1996), The initial cooling of pahoehoe flow lobes, Bull. Volcanol., 58, 5– 18.

Kiyoshi Honda, Masahiko Nagai,2002. ISPRS Journal of Photogrammetry and Remote Sensing Volume 57, Issues 1-2, , Pages 159-168

Losso, Corgnati, Perona 2011. False alarm reduction in a forest fires detection with low-cost commercial sensor. Italian journal of remote sensing. Vol. 43 (1). ISSN 1129-8596

Losso A., Corgnati L.,Perona G. 2010. Innovative image geo-referencing tool for decision support in wildfires fight. Forest Fires II, Kos, Greece.

Malin, M.C. (1980), Lengths of Hawaiian flows, Geology 8, 306–308. Miyamoto, H., e S. Sasaki (1997), Simulating lava flows by an improved cellular automata method, Comput. Geosci., 23, 283–292.

Miyamoto, H. e S Sasaki, (1998), Numerical simulations of flood basalt lava flows: roles of some parameters on lava flow morphologies, J. Geophys. Res., 103, 27 489–27 502.

Neri, A. (1998), A local heat transfer analysis of lava cooling in the atmosphere: Application to thermal diffusion-dominated lava flows, J. Volcanol. Geotherm. Res., 81, 215– 243.

Oppenheimer, C., and G. Yirgu (2002), Thermal imaging of an active lava lake; Erta 'Ale Volcano, Ethiopia, Int. J. Remote Sens., 23, 4777 – 4782.

Patrick, M.R., J. Dehn, e K. Dean (2004), Numerical modeling of lava flow cooling applied to the 1997 Okmok eruption: Approach and analysis, J. Geophys. Res., 109, B03202, doi:10.1029/2003JB002537.

SunJae Ham; ByoungChul Ko; JaeYeal Nam 2010. Fire-Flame Detection Based on Fuzzy Finite Automation,istanbul ISSN: 1051-4651 Print ISBN: 978-1-4244-7542-1

Takahashi and *Shoji*, 2002. *Distribution* and *classification* of *volcanic ash* soils, Global Environmental Research 6.

Tallarico, A., e M. Dragoni (2000), A three-dimensional Bingham model for channeled lava flows, J. Geophys. Res., 105, 25,969–25,980.

Turgay Çelik, Hüseyin Özkaramanlı, and Hasan Demirel 2007. FIRE AND SMOKE DETECTION WITHOUT SENSORS: IMAGE PROCESSING BASED APPROACH. 15th European Signal Processing Conference (EUSIPCO 2007), Poznan, Poland, September 3-7, 2007, copyright by EURASIP.

Wadge, G. e Lopes, R.M.C. (1991), The lobes of lava flows on Earth and Olympus Mons, Mars, Bulletin of Volcanology, 54, 10-24.

Wang, W. (2008). An intelligent system for machinery condition monitoring. IEEE Transactions on Fuzzy Systems,16, 110-122.

Yamanoia ,Takeuchi 2008. Color measurements of volcanic ash deposits from three different styles of summit activity at Sakurajima volcano, Japan: Conduit processes recorded in color of volcanic ash.

Journal of Volcanology and Geothermal Research Volume 178, Issue 1, 30 November 2008, Pages 81-93.

Yuan Wei , Yu Chunyu, Zhang Yongming 2009. Based on wavelet transformation fire smoke detection method, Electronic Measurement & Instruments, 2009. ICEMI '09. 9th International Conference on 16-19 Aug. 2009, Beijing